Eurasian Journal of Physics and Functional Materials

Volume 9 | Number 1

Article 5

Pages: 37 - 47

3-29-2025

High-temperature exciton-like luminescence in KCl:Na crystals

K. Shunkeyev
“Radiation Physics of Materials” Scientific Center, K. Zhubanov Aktobe Regional University, 34 A. Moldagulova Ave., Aktobe 030000, Kazakhstan

Sh. Sagimbayeva
“Radiation Physics of Materials” Scientific Center, K. Zhubanov Aktobe Regional University, 34 A. Moldagulova Ave., Aktobe 030000, Kazakhstan, sh.zh.sagimbaeva@gmail.com

A. Kenzhebayeva
“Radiation Physics of Materials” Scientific Center, K. Zhubanov Aktobe Regional University, 34 A. Moldagulova Ave., Aktobe 030000, Kazakhstan

Yu. Zorenko
Department of Physics, Kazmierz Wielki University in Bydgoszcz, Powstańców Wielkopolskich str., 2, 85-0906 Bydgoszcz, Poland

Recommended Citation

Shunkeyev, K.; Sagimbayeva, Sh.; Kenzhebayeva, A.; and Zorenko, Yu. (2025) "High-temperature exciton-like luminescence in KCl:Na crystals," *Eurasian Journal of Physics and Functional Materials*: Vol. 9: No. 1, Article 5.
DOI: https://doi.org/10.69912/2616-8537.1240

ORIGINAL STUDY

High-temperature Exciton-like Luminescence in KCl:Na Crystals

Kuanyshbek Shunkeyev [a], Shynar Sagimbayeva [a,*], Adelya Kenzhebayeva [a], Yuriy Zorenko [b]

[a] "Radiation Physics of Materials" Scientific Center, K. Zhubanov Aktobe Regional University, 34 A. Moldagulova Ave., Aktobe 030000, Kazakhstan
[b] Department of Physics, Kazmierz Wielki University in Bydgoszcz, Powstańców Wielkopolskich str., 2, 85-0906 Bydgoszcz, Poland

Abstract

The emission spectra of high-temperature peaks of thermally stimulated luminescence (TSL) in the 300 K → 800 K range have been recorded in KCl:Na crystals for the first time. In KCl:Na (1000 ppm), a prominent TSL peak at 575 K has been identified, featuring luminescence bands peaking at 2.8 eV and 3.1 eV, attributed to radiative recombination of excitons bound with single and pair sodium based centers. This effect persists after the thermal treatment of KCl:Na crystals through high-temperature annealing, which ensures the central positioning of sodium ions in the lattice sites of cations, as confirmed by X-ray and tunnel luminescence spectra.

Calculations of temperature-dependent jump frequencies of vacancies reveal that cation vacancies predominantly contribute to the breakdown of halide formations in the Type I TSL peaks (400 K) region, while at consideration of nature for the Type II peaks (555 K), the involvement of anion vacancies must also be taken into account.

The thermal dissociation of halide formations, driven by the mobility of both cation and anion vacancies in KCl:Na (1000 ppm), generates a flux of non-relaxed holes (e^+), which recombine with electrons (e^-) in the field of sodium ions. As a result of such recombination, high-temperature exciton-like luminescence $(e^0_{SL}(Na^+_c))$ is produced with a maximal light yield at 575 K. The last property is particularly relevant for temperature stable scintillation detectors and dosimeters.

Keywords: Alkali halide crystals, High-temperature thermally stimulated luminescence, X-ray luminescence, Tunnel luminescence, High-temperature exciton-like luminescence

1. Introduction

In alkali halide crystals (AHCs), there is a unique opportunity to sequentially investigate the efficiency of luminescence yield and radiation defect formation, both directly linked to decay of self-trapped excitons (STE) [1,2]. Such studies are driven by vigorous innovation of both scintillators and dosimeters for detecting ionizing radiation, exemplified by LiF crystals [3—7].

Fundamentally, thermally stimulated luminescence (TSL) phenomena is based on electron-hole recombination luminescence of radiation defects, arising during linear heating of a pre-irradiated crystal. Due to the tissue-equivalent properties of LiF to gamma radiation, dosimeters on the base of this materials with intensive TSL are applied in radiation therapy, radiobiology, and shielding in nuclear reactors [7—12]. Namely, high-temperature TSL peaks of LiF crystals with maxima at 473 K (TLD-100) and 490 K (TLD-700H) serve as the primary dosimetric indicators [6—8,13—16].

Strategic use of innovative functional materials, such as cryodetectors and nanotubes of different shapes and sizes [17—20], also motivates preliminary investigations under conditions of deliberate symmetry reduction in the lattice caused by local [21—23], uniaxial [24—27], and hydrostatic deformations [28—30].

Currently, the delocalization temperatures of self-trapped holes (V_K-centers, X_2^- dihalogen molecules

Received 14 February 2025; revised 24 February 2025; accepted 24 February 2025.

---

* Corresponding author.
E-mail address: sh.zh.sagimbaeva@gmail.com (S. Sagimbayeva).

https://doi.org/10.69912/2616-8537.1240

[31,32]) are established for all AHCs, and their mobility and interactions with other radiation defects lead to recombination luminescence [2,21–23,33]. The analyses of experimental studies [2,19–23,31–35] reveals that in alkali metal chlorides, the decrease of V_K-center delocalization temperatures (indicated in parentheses) correlates with the decreasing cationic radii in the row NaCl (168 K) → KCl (208 K) → RbCl (240 K).

Generally, low-temperature TSL AHCs in 85 K→300 K range arises from the recombination of thermally delocalized (mobile) hole defects (the so-called V_K-center family) with electron-type defects—F-centers (anion vacancies with one captured electron – $\upsilon_a^+ e^-$) [2,21–23,33]. The V_K-center family also includes holes localized to the vicinity of cation vacancies – $V_F = \upsilon_c^+ e^+$; and holes localized with the single Na^+ dopant, isoelectronic to host K^+ cations – $V_{KA} = e^+(Na^+)$, or with pair dopants $V_{KAA} = e^+(Na^+, Na^+)$. The structure of the $V_F = \upsilon_c^+ e^+$-center is interpreted as an anti-F-center ($\upsilon_a^+ e^-$). The indices A in the designations V_{KA} and V_{KAA} denote single and paired Na^+ dopants.

Complementary pairs of $V_2 = (X_3^-)_{aca}$- and F-centers are stable radiation defects in AHCs above room temperature, and their thermal annealing is accompanied by TSL in the range of 365–420 K [21–23,33,36]. Moreover, the increase of the anion-to-cation radii ratio, result in the lower temperature of the corresponding TSL peak [21–25,33,36] in KI (365–370 K), KBr (375–385 K), KCl (90–400 K) and NaCl (400–420 K).

This work continues the research on high-temperature TSL peaks in AHCs [38]. Despite the extensive study [21–25,33,37] of KCl crystals (both pure and doped), the emission spectra of the high-temperature TSL peaks in the temperature range from 300 K up to 800 K, corresponding to the complete discoloration of radiation defects, have not been registered yet. In this regard, the spectral composition of high-temperature TSL peaks in KCl:Na crystals was investigated for the first time in this work, in order to explain the mechanism of recombination luminescence of radiation defects activated by sodium ions.

2. Materials and methods

KCl and KCl:Na crystals were synthesized at the Institute of Physics of University of Tartu, Estonia, using the Stockbarger method in vacuum-sealed quartz ampoules [38].

The growth of KCl crystals followed an extensive purification process of the raw material, which included: (i) vacuum drying of powdered KCl at 80–100 °C to eliminate oxygen-containing impurities (OH); (ii) chlorine gas treatment of the KCl melt to remove bromine impurities in gaseous form; (iii) multiple recrystallization, i.e., “zone refining” of the raw KCl. Such purification technique allow to produce the crystals with minimal concentrations of uncontrolled impurities, confirmed by flame photometry to be within the range of 0.01–1.0 ppm.

Doped KCl:Na crystals were grown using zone-refined KCl material combined with NaCl powder, which had undergone the aforementioned purification protocol. The concentrations of sodium ions in the charge were 100 ppm, 1000 ppm, and 10,000 ppm, while the actual concentrations in the resulting KCl:Na crystals, accounting for the sodium incorporation coefficient ($k = 0.11$), were 10 ppm, 100 ppm, or 1000 ppm, which is consistent with flame photometry data.

Prior to experimental use, the doped KCl:Na crystals underwent additional thermal quenching to ensure homogeneous distribution of sodium ions within the lattice (details in Refs. [21–23]). This process involved heating the crystals to 650–700 °C at a rate of 15 °C/min in a Programix TX 25 electric muffle furnace (Ugin-Dentaire), holding them at the target temperature for 15 minutes, and then rapidly cooling them on a quartz substrate to room temperature.

Radiation-induced defects were generated at ambient temperature by exposing the crystals to bremsstrahlung X-rays from the RUP-120 (W-anticathode, 3 mA, 100 kV) at an exposure dose of 10 mGy, which, unlike characteristic X-rays, ensures uniform defect distribution throughout the crystal thickness (1.0–1.3 mm).

High-temperature TSL measurements were performed during controlled heating at a constant rate ($\beta = 5.0$ K/s) in the 300–850 K range using Harshaw Model 3500, an automated thermoluminescent dosimeter setup equipped with WinREMS software.

Emission spectra of high-temperature TSL, as well as XRL and TL, were acquired during heating ($\beta = 5.0$ K/s) in a quartz furnace. Scanning of TSL spectra were conducted in the range of 1.8–6.0 eV using an MSD-2 high-aperture monochromator, an H8259 photomultiplier tube (Hamamatsu), and the SpectraScan software.

The “thermally stimulated luminescence (TSL)” term is employed due to its more accurate reflection of the phenomenon's physical essence, as proposed by Ch. Lushchik [33], instead of “thermoluminescence (TL)”, widely accepted in dosimetry. Additionally, in this study, TL refers to tunnel luminescence, necessitating a clear distinction to avoid confusion.

To ensure accurate comparisons of TSL light yield of the studied crystals, their dimensions and X-ray exposure levels were meticulously considered. The integral light yield (S), defined as the area under the TSL curve, served as the metric for evaluating TSL efficiency.

3. Results and discussion

3.1. High-temperature TSL of KCl and degraded KCl:Na crystals

In KCl:Na crystals, the efficiency of forming sodium-related halogen radiation defects, $I_A(\mathrm{Na}^+)$- and $H_A(\mathrm{Na}^+)$- centers, corresponding to near-sodium interstitial ions $I_A(\mathrm{Na}^+)$ and atoms $H_A(\mathrm{Na}^+)$ of chlorine, as well as the exciton-like formations, $e^0_{\mathrm{SL}}(\mathrm{Na}^+)$ and $e^0_{\mathrm{SL}}(\mathrm{Na}^+, \mathrm{Na}^+)$ have been demonstrated using absorption [21] and luminescence [22] spectroscopy methods. It was established that sodium impurity ions, initially occupying regular cationic sites in as-grown crystals, gradually migrate and form nanoscale clusters. The indicators of sodium ion instability in the KCl:Na lattice [21,22] are absorption bands at 6.3 and 3.5 eV, corresponding to $I_A(\mathrm{Na}^+)$ and atoms $H_A(\mathrm{Na}^+)$ centers, as well as luminescence bands at 2.8 and 3.1 eV, associated with exciton-like formations near isolated $e^0_{\mathrm{SL}}(\mathrm{Na}^+)$ and paired $e^0_{\mathrm{SL}}(\mathrm{Na}^+, \mathrm{Na}^+)$ sodium ions.

Based on the above experimental findings [21,22], it can be concluded that in degraded KCl:Na crystals, sodium ions (irrespective of concentration) become optically inactive, i.e. look like “absent” from the lattice. To verify this, high-temperature TSL peaks (Fig. 1) were recorded for reference pure KCl crystals, containing minimal content (up to 1 ppm) of trace impurities, and for KCl:Na (1000 ppm) crystals stored long-term in a vacuum desiccator at room temperature, which are categorized as degraded samples.

Numerous experimental results [21,38] indicate that high-temperature TSL peaks in AHCs primarily occur in the 365—400 K and 520—620 K temperature ranges, designated as TSL peaks of Type I and Type II, respectively. In KCl crystals, $V_2 = (X_3^-)_{aca}$-centers [21—23,33,36], which are three-halide formations occupying two anionic and one cationic sites in the lattice, correspond to TSL peak of Type I. Apparently, TSL peak of Type II at 520—620 K arise from (Cl_n^-) polyhalide formations, which larger than (Cl_3^-)-centers.

Fig. 1 shows the high-temperature TSL peaks of the studied samples under identical experimental conditions (crystals’ dimensions, irradiation dose and temperature, heating rate). It reveals only a slight increase in TSL intensity for peaks at 374 K, 515 K, and 560 K in KCl:Na (1000 ppm, curve 2) compared to reference undoped KCl crystal (curve 1), despite more than a 1000-fold difference in Na concentrations in these samples (see also Materials and Methods).

Detailed comparison of the TSL peaks (curves 1 and 2 in Fig. 1) suggests that in degraded KCl:Na crystals, Na based centers, become absolutely “inactive” despite their high concentration, characteristic of their

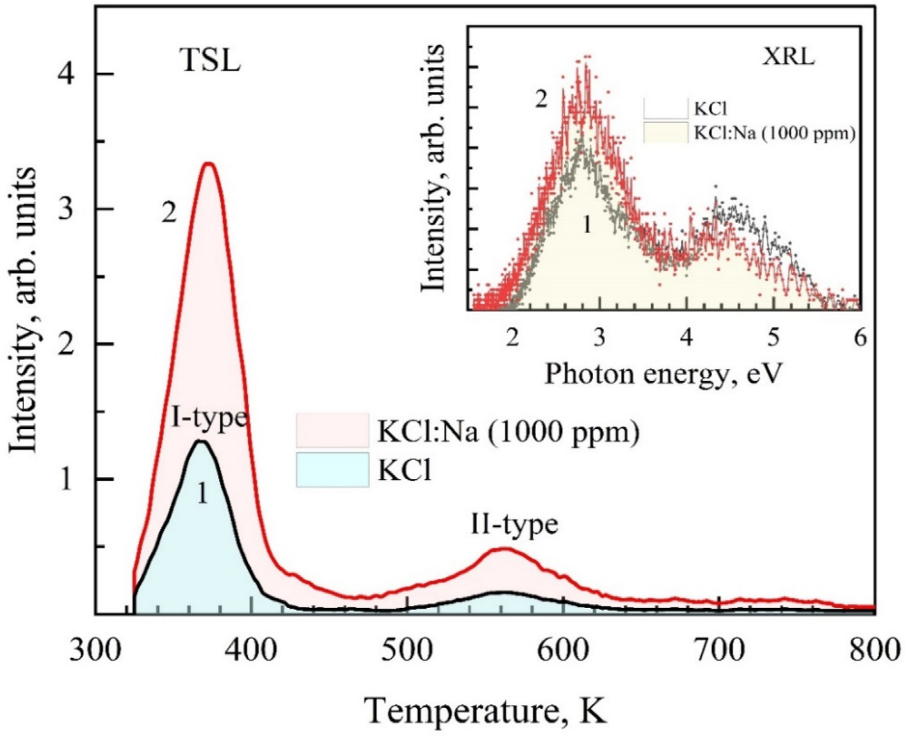

Fig. 1. Thermally stimulated luminescence (TSL) of reference pure KCl crystal (curve 1) and “degraded” KCl:Na crystal (1000 ppm, curve 2) after X-ray irradiation (10 mGy) at room temperature (RT). Inset: X-ray luminescence (XRL) spectra of KCl (curve 1) and “degraded” KCl:Na (1000 ppm, curve 2) crystals recorded at RT.

displacement from cationic lattice sites. It appears that the slight increase in TSL intensity in KCl:Na (curve 2 in Fig. 1) arises from a negligible number of remaining sodium ions in the cationic lattice sites.

This prompted us to detect the presence of impurities in the KCl matrix as exciton-like luminescent formations via recording XRL spectra shown in the inset of Fig. 1. The primary conclusion from analysis of the XRL spectra of KCl crystal (curve 1 in the inset) and KCl:Na crystal (curve 2 in the inset) is that their spectral composition is nearly indistinguishable, remaining at background levels. This also suggests the absence of impurities, even those introduced in significant concentrations (above 5000 ppm). Own luminescence of KCl crystals is characterized by radiative relaxation of STEs with a π-luminescence band peaking at 2.3 eV, which can only be observed at 4.2 K due to the absence of thermal quenching. As the temperature increases, the π-luminescence of STE undergoes rapid thermal quenching, becoming fully bleached above 40 K.

Consequently, in the XRL spectra of KCl recorded at 300 K (curve 1 in the inset of Fig. 1), π-luminescence of STE is absent, and only weak, non-elementary emissions are observed in the 2.4—3.5 eV and 4.0—5.0 eV regions, likely attributed to *complex defects and/or trace impurity centers.* According to the literature [2,3,39—42], these spectral regions in KCl host are associated with thermally stable emissions of exciton-like formations localized near single anion vacancies (α-luminescence with a maximum at 2.65 eV) or divacancies (d-luminescence with a maxima at 3.1 eV, 3.4 eV, and 3.8 eV). Even in reference-grade KCl crystals subjected to deep purification (see Materials and Methods), traces of homologous impurity cations remain, responsible for exciton-like luminescence in the 2.8 eV region. Thus, based on TSL and XRL data, it can be inferred that in degraded KCl:Na crystal, sodium ions become inactive such as luminescent centers due to their displacement from central positions in the cationic lattice sites [21,22].

Further experiments involving registration of high-temperature TSL peaks and the TSL and XRL spectra were conducted using annealed KCl:Na (1000 ppm) crystal to ensure homogeneous sodium ion distribution (details in Refs. [21,22]). The annealing procedure is described in Materials and Methods, and subsequent experiments were performed with annealed KCl:Na (1000 ppm) crystal. In contrast to unannealed sample (Fig. 1, curve 2), annealed KCl:Na (1000 ppm) crystal exhibit TSL peaks (Fig. 2) at 400 K (1), 430 K (2), 480 K (3), 570 K (4), and 660 K (5). The TSL peaks are numbered sequentially as they appear during heating at a constant rate, from to three-halide (Type I) to polyhalide (Type II) formations.

Table 1 presents the integral light sumы (S) for TSL of three crystals: S_a for KCl (taken as a unit), S_b for degraded KCl:Na (1000 ppm), and S_c for annealed

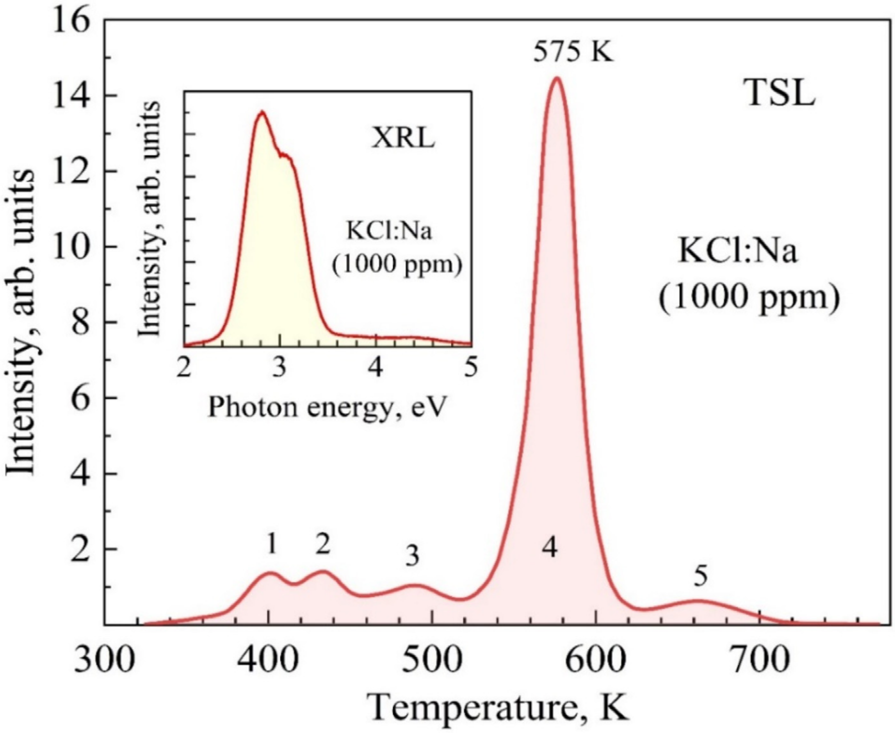

Fig. 2. TSL and XRL spectra (inset) of annealed KCl:Na (1000 ppm) crystal after uniform (10 mGy) X-ray irradiation at RT.

Table 1. Comparative analysis of integral light sums (S) and activation energies (E_a) of TSL peaks in KCl, KCl:Na (1000 ppm, degraded), and KCl:Na (1000 ppm, annealed) crystals.

Crystals	*S* arb. units	$\frac{S_n}{S_a}$	E_a, eV Type *I* TSL	E_a, eV Type *II* TSL
KCl	$S_a = 2.1$	1	0.71	1.6
KCl:Na(1000 ppm, degraded)	$S_b = 6.5$	3	0.8	1.72
KCl:Na (1000 ppm, annealed)	$S_c = 720$	343	1.3; 1.35; 1.5	2.2; 2.4

KCl:Na (1000 ppm), along with the activation energies (E_a) of the TSL peaks. According to Table 1, annealed KCl:Na (1000 ppm) crystals exhibit the highest *S* value, with a ratio of $S_c/S_a = 343$.

From Table 1, it can be observed that E_a for Type I TSL peaks, calculated using the Lushchik formula [33,38], range from 0.71 to 1.5 eV, while those for Type II TSL peaks are higher, from 1.6 to 2.4 eV.

On that account, the presence of sodium ions in the cationic lattice sites, restored through high-temperature annealing of KCl:Na (1000 ppm) crystals, remarkably enhances ($S_c/S_a = 343$) the high-temperature TSL peaks (Type II) with maxima at 575 K, making them suitable for using as dosimetric indicators in detectors.

The intense XRL spectrum with maxima at 3.1 eV and 2.8 eV, shown in the inset of Fig. 2, also confirms the central position of sodium ions in the cationic lattice sites after annealing of the KCl:Na (1000 ppm) crystal.

A comparative analysis of the TSL and XRL spectra of unannealed KCl:Na (1000 ppm) and the same crystal post-annealing (Fig. 2, curves 1 and 2, respectively) demonstrates that thermal treatment reinstates sodium ions back into the lattice. This restoration results in an increased concentration of electronic excitations under X-ray irradiation.

This conclusion is supported by the simultaneous enhancement of XRL and TSL intensities (Fig. 2) under uniform X-ray exposure of the annealed KCl:Na (1000 ppm) crystal. According to the fundamental principles of electronic excitation decay, in AHCs, an increase in luminescence yield (in this case, XRL) corresponds to a reduction in the efficiency of radiation defect formation (in this case, TSL), or vice versa, as both of these processes are governed by STEs decay [2,33].

3.2. Spectra of high-temperature TSL of annealed KCl:Na crystals

In order to study the products of the thermal dissociation of halide formations that manifest as recombination luminescence in greater detail, we recorded spectra at the high-temperature TSL peaks (Fig. 2).

Scanning the TSL spectra in the range from 2.0 eV to 4.0 eV was performed over 6 seconds at 50 nm/s while heating the crystal at a constant rate of $\beta = 1.5$ K/s, corresponding to the sample temperature change of approximately 10 K. Considering that the half-widths of high-temperature TSL peaks are approximately 20 K (Type I) and 50 K (Type II), it was feasible to perform multiple scans of the TSL spectra during the crystal's luminescence decay. To minimize time loss, the process was initiated before the TSL peak maximum was reached, ensuring that scanning was carried out at the peak maximum.

Fig. 3 shows the normalized TSL spectra of the annealed KCl:Na (1000 ppm) crystal, recorded at the peaks identified in Fig. 2: *a* — at 400 K (1), 430 K (2), and 490 K (3); *b* — at 575 K (4); *c* — at 660 K (5). The TSL peaks at 400 K (1), 430 K (2), and 490 K (3) in the KCl:Na (1000 ppm) crystal exhibit relatively weak intensities (peaks 1, 2, and 3 in Fig. 2). Their spectra are correspondingly weak and repetitive, so they can be represented by a single characteristic spectrum consisting of two luminescence bands, as shown in Fig. 3*a*.

In the temperature range of the dominant TSL peak at 575 K (peak 4 in Fig. 2), the TSL spectra reveal intense bands (Fig. 3*b*) with maxima at 3.1 eV and 2.8 eV (FWHM Δ equal to 0.38 eV and 0.36 eV, respectively).

The spectrum of the highest-temperature TSL peak (660 K) consists of two emission bands with maxima at 3.1 eV and 2.8 eV.

It is important to note that the low intensity of the TSL peaks at 400 K (1), 430 K (2), 490 K (3), and 660 K (5) resulted in less precise spectral measurements. Nevertheless, overall shapes of the emission bands in these peaks remain unchanged.

Analysis of the TSL spectra of KCl:Na (1000 ppm) crystals reveals intensity ratios of 0.1:1.0:0.05 (Fig. 3), which are consistent with the integral TSL intensities (Fig. 2).

The entire integral light sum of TSL in the KCl:Na crystals can be attributed to two luminescence bands at 3.1 eV and 2.8 eV, whose origin is also associated with sodium impurities [21].

To determine the nature of luminescence based on TSL spectra, it is essential to understand the dissociation products of halide formations. Electrons released from *F*-centers during recombination with dissociation products near sodium ions generate high-temperature exciton-like luminescence.

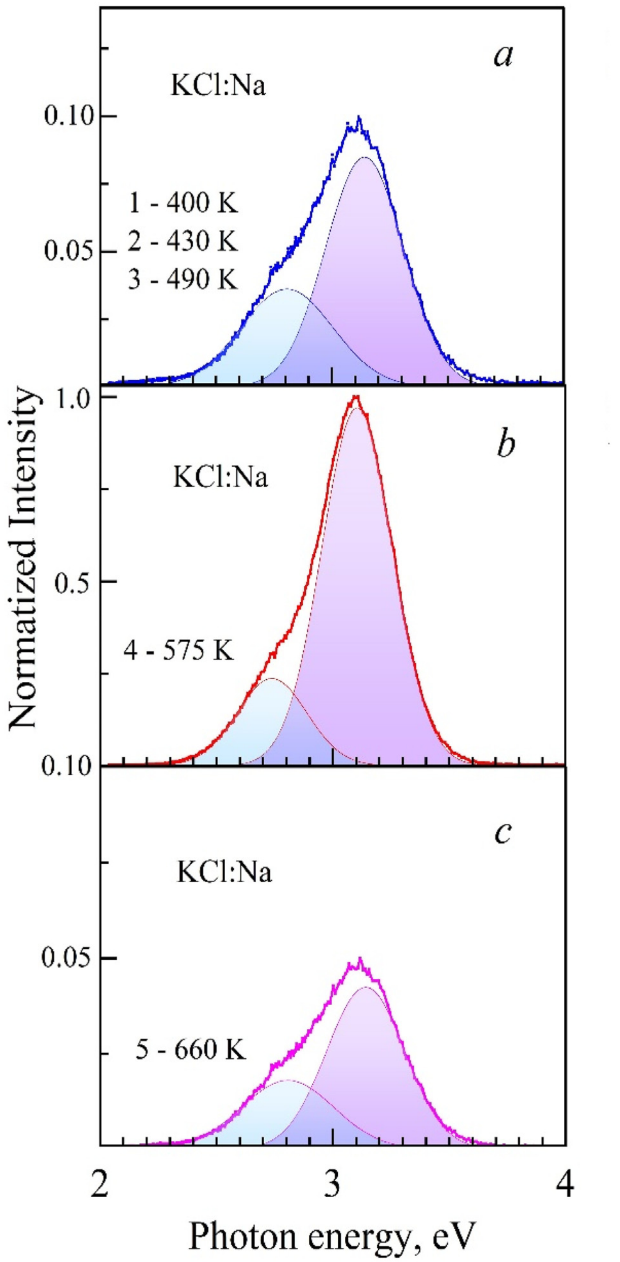

Fig. 3. TSL spectra of the annealed KCl:Na (1000 ppm) crystal recorded at the peaks identified in Fig. 2: a — at 400 K (1), 430 K (2), and 490 K (3); b — at 575 K (4); c — at 660 K (5). The TSL and TSL spectra were simultaneously recorded through two luminescence detection channels described in Materials and Methods.

It is known that in KCl crystals [21,22,33,36,43—46], the thermal dissociation of elementary three-halide V_2-centers occurs in the temperature range of 380—400 K, with the dissociation products being mobile holes (e^+) and interstitial halogen atoms (i_a^0, H-centers):

$$V_2+T,\mathrm{K} \rightarrow (V_2)^* \rightarrow e^+ \ldots v_c^- \ldots i_a^0 \rightarrow e^+. \quad (1)$$

According to reaction (1), thermal dissociation of V_2-centers in KCl produces a flux of mobile holes with a mean free path of up to $1000a$ (where a is the lattice constant) [34,47]. These holes may interact with F-centers or localise around sodium impurity ions: $e^+ \rightarrow e_S^+(Na_c^+)$. Consequently, during thermal dissociation of (Cl_n^-) polyhalide quasi-molecules, a flux of mobile holes is reasonable to expect, with larger formations leading to higher concentrations of non-relaxed holes. In other words, during this process, polyhalide quasimolecules become a source of non-relaxed holes.

In KCl crystals, thermal dissociation (ionisation) of F-centers occurs at the same time with thermal dissociation of V_2-centers within the same temperature range of 380—400 K, following the scheme:

$$F+T,K \rightarrow \left(v_a^+ e^-\right)^* \rightarrow v_a^+ \ldots e^- \rightarrow e^-. \quad (2)$$

According to (2), thermal ionisation of F-centers releases free electrons, which are likely to interact (due to their charges) with self-trapped holes in the sodium field. As a result, an exciton-like state of electronic excitation forms in KCl:Na crystals [21—23], radiatively relaxing in the sodium field, with maxima at 3.1 eV and 2.8 eV:

$$e^- + e_S^+\left(\mathrm{Na_c^+}\right) \rightarrow e_{SL}^0\left(\mathrm{Na_c^+}\right) \rightarrow h\nu\,(2.8\,\mathrm{eV}); \quad (3)$$

$$e^- + e_S^+\left(\mathrm{Na_c^+},\mathrm{Na_c^+}\right) \rightarrow e_{SL}^0\left(\mathrm{Na_c^+},\mathrm{Na_c^+}\right) \rightarrow h\nu\,(3.1\,\mathrm{eV}). \quad (4)$$

Here, $e_{SL}^0\left(\mathrm{Na_c^+}\right)$ and $e_{SL}^0\left(\mathrm{Na_c^+},\mathrm{Na_c^+}\right)$ denote exciton-like formations localised near single and paired sodium ions, respectively, with the subscript "c" indicating the cationic lattice site occupied by sodium, and the superscript "+" indicating charge relative to the lattice.

X-ray irradiation facilitates the predominant formation of electron-hole pairs in the crystal, which recombine in regions of localized lattice deformation induced by light impurity cations (e.g., Na in KCl), producing exciton-like formations near impurity ions [21—23]. In this regard, comprehensive comparison of the TSL, XRL and TL spectra of KCl:Na crystals (1000 ppm) was carried out and presented in Figs. 3 and 4.

A comparative analysis of TSL spectra at the 575 K peak (Fig. 3*a*), XRL spectra (Fig. 4*a*), and TL spectra (Fig. 4*c*) of KCl:Na (1000 ppm) crystals reveals several patterns. Firstly, all emission bands share identical maxima at 3.1 eV and 2.8 eV, corresponding to the radiative relaxation of exciton-like formations in the field of sodium ions [21—23,34]. Secondly, the spectra differ in emission band widths: the TSL spectrum at the 575 K peak (Type II) has broader half-widths $\Delta_1 = 0.38$ eV (3.1 eV) and $\Delta_2 = 0.36$ eV (2.8 eV) compared to the narrower XRL and TL spectra

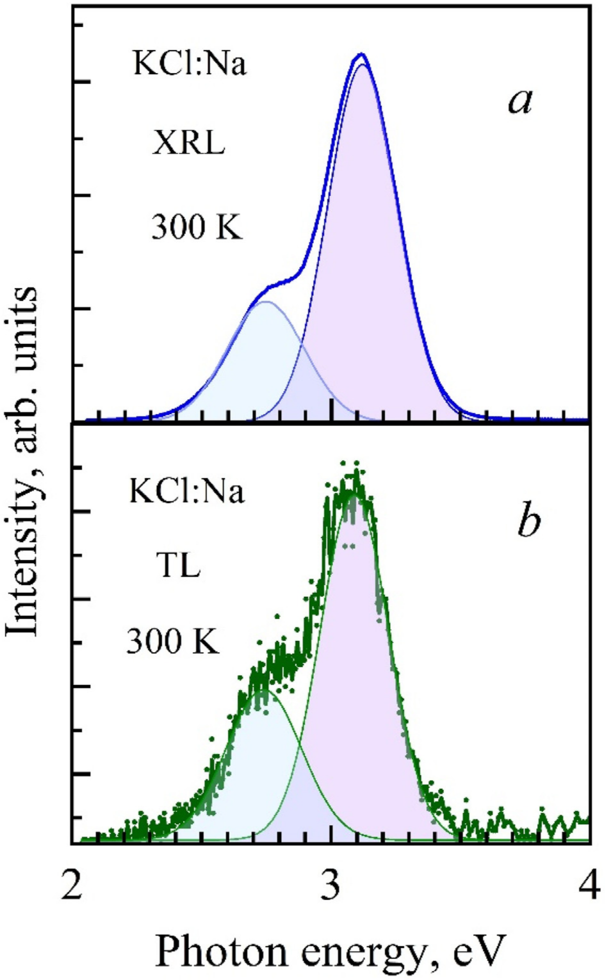

Fig. 4. TSL spectra at the 575 K peak (a), XRL spectra (b), and TL spectra (c) of KCl:Na (1000 ppm) crystals. XRL and TL spectra were measured at 300 K. Thin solid lines represent the decomposition into elementary Gaussians.

($\Delta_1 = 0.32$ eV (3.1 eV) и $\Delta_2 = 0.34$ eV (2.8 eV)). This narrowing of XRL and TL luminescence bands relative to the TSL spectrum at 575 K is quite consistent with electron-phonon interaction, as XRL spectra were recorded at 300 K, while TSL spectra were obtained in the 565–585 K temperature range, much higher than 300 K.

Thus, in KCl:Na crystals, the spectral similarity between TSL, XRL, and TL in the 400–660 K temperature range demonstrates that they share the same luminescence origin with maxima at 3.1 eV and 2.8 eV.

Extensive experimental data (concentration, temperature, deformation dependencies) confirm [21–23,34] that the luminescence spectrum with maxima at 3.1 eV and 2.8 eV arises from the radiative relaxation of exciton-like formations near sodium ions ($r(\mathrm{K}^+)/r(\mathrm{Na}^+) = 1.35$) that form through the recombination of electron-hole pairs created by X-ray irradiation. The creation of exciton-like formations in KCl:Na crystals during TSL spectra registration is facilitated by the flux of mobile holes released during the thermal dissociation of polyhalide defects and their recombination with electrons near sodium impurity ions, according to reactions (3) and (4).

3.3. Temperature dependence of vacancy frequency jumps in KCl and KCl:Na crystals

When analysing the nature of high-temperature TSL peaks, in addition to direct recombination of complementary radiation defects, one must consider the migration of anion and cation vacancies, which facilitates the breakdown of complex polyhalide formations in KCl single crystals [2,21–23,48–50]. In this context, we calculated the temperature dependence of the jump frequencies for cation $\nu\ (\upsilon_c^-)$ and anion $\nu\ (\upsilon_a^+)$ vacancies in the KCl crystalline lattice using the formula from Ref. [49]:

$$\nu\ (\upsilon_c^-) = \nu_0 \exp\left(\frac{S(\upsilon_c^-)}{k_\mathrm{B}}\right) \exp\left(-\frac{E_a(\upsilon_c^-)}{k_\mathrm{B}T}\right); \qquad (5)$$

$$\nu(\upsilon_a^+) = \nu_0 \exp\left(\frac{S(\upsilon_a^+)}{k_\mathrm{B}}\right) \exp\left(-\frac{E_a(\upsilon_a^+)}{k_\mathrm{B}T}\right). \qquad (6)$$

$S\ (\upsilon_c^-)$, $S\ (\upsilon_a^+)$ are the respective entropies of cation and anion vacancies' migration. $E_a\ (\upsilon_c^-)$, $E_a\ (\upsilon_a^+)$ are the respective migration activation energies, ν_0 is Debye frequency, k_B is Boltzmann's constant.

The thermal activation parameters required for calculations, determined for KCl crystals in Ref. [49], are summarized in Table 2.

Fig. 5 shows the calculated temperature dependences of vacancies' jump frequencies in KCl and KCl:Na crystals. The onset of mobility is defined as the temperature at which a vacancy performs one jump per second, $\nu = 1\ \mathrm{s}^{-1}$. Negative values on the ordinate axis represent the temperature range where vacancies remain immobile (localized). The mobility onset

Table 2. Thermal activation characteristics of KCl crystals [49].

Crystall	ν_0, s^{-1}	Cation vacancy, υ_c^-			Anion vacancy, υ_a^+		
		T for $\nu\ (\upsilon_c^-) = 1$, K	$E(\upsilon_c^-)$, eV	$\frac{S\ (\upsilon_c^-)}{k_B}$	T for $\nu(\upsilon_a^+) = 1$, K	$E(\upsilon_a^+)$, eV	$\frac{S\ (\upsilon_a^+)}{k_B}$
KCl	4.25×10^{12}	270	0.73	2.4	307	0.85	3.2

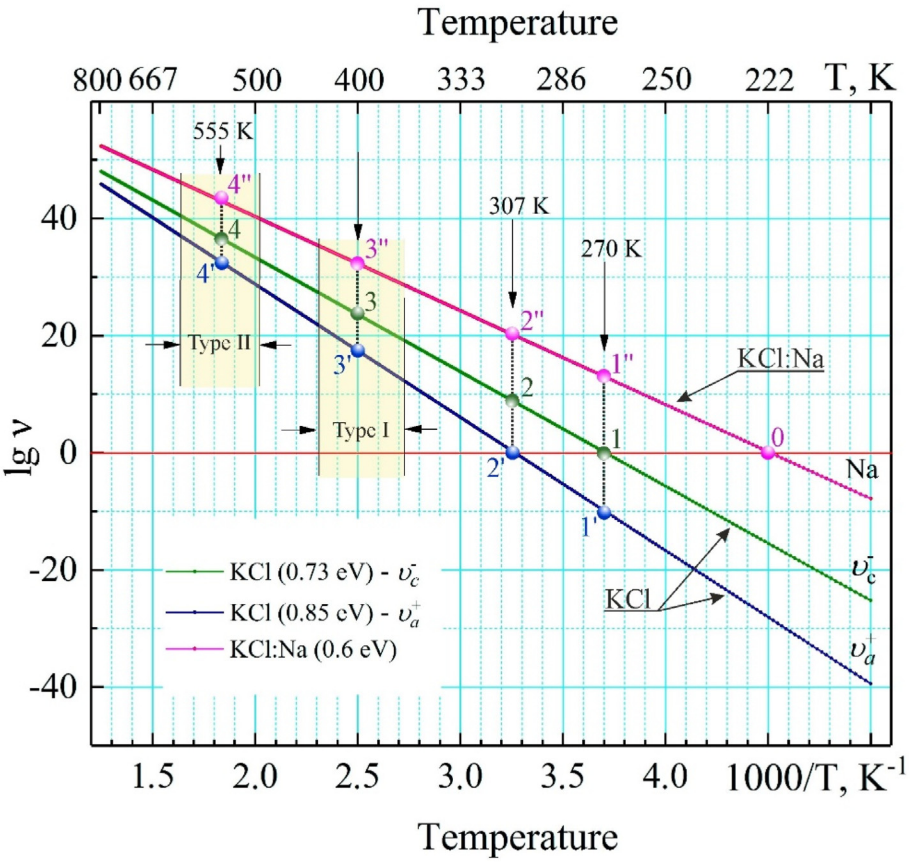

Fig. 5. Temperature dependence of cation and anion vacancies' jump frequencies in KCl and KCl:Na crystals. Highlighted in yellow are temperature ranges corresponding to Type I (360–425 K) and Type II (495–620 K) TSL peaks. By the red horizontal line the threshold jump frequency ($\lg\nu = 0$) is marked. Numbers on the graph indicate specific temperature points associated with vacancy mobility in the studied crystals: 0–222 K; 1, 1', 1" – 270 K; 2, 2', 2"– 307 K; 3, 3', 3" – 400 K и 4, 4', 4" – 555 K.

temperatures ($\nu = 1$) for υ_c^- and υ_a^+ in KCl are 270 K and 307 K, respectively (points 1 and 2' in Fig. 5). As shown in Table 4, at the onset of anion vacancy diffusion ($\nu(\upsilon_a^+) = 1$), cation vacancies in KCl are already highly mobile: $\nu(\upsilon_c^-) = 46$ s^{-1}. According to Fig. 5, at 270 K and 307 K (points 1→2) only cation vacancies are mobile ($\lg\nu(\upsilon_c^-) > 0$) in KCl.

The results of thorough comparison of jump frequencies for cation and anion vacancies in KCl and KCl:Na crystals across different temperature ranges (derived from Fig. 5) are summarized in Table 3. The data highlight temperature ranges corresponding to Type I and Type II TSL peaks (highlighted areas marked by points 3 and 4 in Fig. 5). Upon surpassing the critical value ($\lg\nu = 0$), which indicate the onset of anion vacancy mobility in KCl, there is a substantial decline in the frequency difference between υ_c^- and υ_a^+. In the Type I TSL region (see data in Table 4 for the centre of the range at 400 K), the ratio $\nu(\upsilon_c^-)/\nu(\upsilon_a^+)$ equals 15. In the Type II TSL region (555 K is chosen), this ratio decreases to 6.

For this reason, in the formation of Type I TSL peaks, much higher agility of υ_c^- in this region can act as a cornerstone contrary to the processes leading to the emergence of TSL peaks of Type II, the involvement of both υ_c^- and υ_a^+ appears equally feasible.

Table 3. Temperature-dependent comparison of cation and anion vacancies' jump frequencies in KCl and KCl:Na crystals (as per Fig. 5).

Crystals	270 K–307 K			Type I TSL 400 K			Type II TSL 555 K		
	$\nu(\upsilon_c^-)$, s^{-1}	$\nu(\upsilon_a^+)$, s^{-1}	$\frac{\nu(\upsilon_c^-)}{\nu(\upsilon_a^+)}$	$\nu(\upsilon_c^-)$, (× 10^4) s^{-1}	$\nu(\upsilon_a^+)$, (× 10^4) s^{-1}	$\frac{\nu(\upsilon_c^-)}{\nu(\upsilon_a^+)}$	$\nu(\upsilon_c^-)$, (× 10^6) s^{-1}	$\nu(\upsilon_a^+)$, (× 10^6) s^{-1}	$\frac{\nu(\upsilon_c^-)}{\nu(\upsilon_a^+)}$
KCl	46	1	46	2.9	0.19	15	11.5	2	6
KCl:Na	2135	1	2135	124.7	0.19	656	162.6	2	81

In KCl:Na crystals doped with impurity ions of smaller ionic radii ($r(K^+)/r(Na^+) = 1.35$), the activation energy for cation vacancy migration within the lattice decreases to 0.6 eV [33,48–50]. It should be recalled that the activation energies of vacancies, depending on the ionic radius of anions (Cl^-) and cations (K^+, Na^+), have decreasing values – 0.85 eV, 0.73 eV and 0.6 eV, which is reflected in their mobility along the KCl:Na crystal lattice [33,49].

Accordingly, the temperature dependence, as also shown in Fig. 5, differs profoundly. As indicated in Table 4, in the KCl:Na crystal, cation vacancies become mobile at 222 K with a frequency of 1 s^{-1} (point 0 in Fig. 5). At 270 K, the vacancy jump frequency reaches 2.8×10^2 s^{-1} (point 1"); at 307 K–6.3×10^3 s^{-1} (point 2"); at 400 K–124.7×10^4 s^{-1} (point 3"); and at 555 K–162.6×10^6 s^{-1} (point 4"). Clearly, these frequencies are substantially higher than those for pure KCl crystals.

Thus, υ_c^- in sodium-doped crystals (KCl:Na) gain mobility even at lower temperatures compared to the pure matrix. In the regions corresponding to TSL peaks of Type I and Type II, the evaluated $\nu(\upsilon_c^-)$ values exceed those $\nu(\upsilon_a^+)$ by nearly an order of magnitude. This highlights the role of υ_c^- in generation of TSL peaks, particularly in the process of polyhalide formations (for example, trihalide quasi-molecules $(Cl_3^-)_{aca}$) and complementary electronic *F*-centers decomposition. It is noteworthy that the high-temperature decomposition of polyhalide molecules generates mobile holes, and recombination with electrons in the vicinity of impurity cations can keep on through exciton-like states (bound excitons), with characteristic emissions observed in the high-temperature TSL spectra.

4. Conclusions

The study of high-temperature TSL peaks in KCl:Na crystals has revealed that the presence of light sodium impurity cations significantly enhances the intensity of integral recombination luminescence of radiation-induced defects at 575 K. This effect was achieved following the regeneration of KCl:Na crystals through high-temperature quenching, ensuring the central positioning of sodium in the cationic lattice sites.

The spectra of high-temperature TSL at 300–800 K have been recorded for the first time for KCl:Na crystals that were X-ray treated at room temperature. An analysis of experimental results demonstrated that, in quenched KCl:Na(1000 ppm) crystals, the high-temperature TSL peaks spectra (with a dominant peak at 575 K) are identical to those of XRL and TL and consist of two luminescence bands with maxima at 2.8 eV ($\Delta_1 = 0.36$ eV) and 3.1 eV ($\Delta_2 = 0.38$ eV).

It is proposed that the observed TSL luminescence bands (2.8 eV and 3.1 eV) result from the radiative decay of exciton-like formations localized around light sodium ions in KCl:Na(1000 ppm) crystals. The formation of such exciton-like states is supported by a stream of non-relaxed holes emitted as thermal dissociation of polyhalide defects takes place (Reaction 1), as well as their recombination with electrons formed via thermal ionisation of *F*-centers (Reaction 2) near sodium ions, as described in Reactions (3) and (4).

Conflicts of interest

The authors declare no conflicts of interest.

Funding

The research work has been funded by Science Committee of the Ministry of Science and Higher Education of the Republic of Kazakhstan (Grant No. AP26100001).

Acknowledgment

We extend our heartfelt thanks to Professor D. Sergeyev for his assistance with the calculations.

References

[1] A.M. Stoneham, N. Itoh, Materials modification by electron excitation, Appl. Surf. Sci. 155 (2000) 186–193, https://doi.org/10.1016/S0169-4332(00)00587-0.

[2] K.S. Song, R.T. Williams, Self-Trapped Excitons, Springer Science & Business Media, 2013. ISBN: 978-3-642-85236-7.

[3] Y. Takizawa, K. Kamada, M. Yoshino, K.J. Kim, N. Kutsuzawa, A. Yamaji, et al., Growth of thallium-doped CsI/CsCl/KCl eutectics and their scintillation properties, Opt. Mater. X 15 (2022) 100159, https://doi.org/10.1016/j.omx.2022.100159.

[4] K. Miyazaki, D. Nakauchi, T. Kato, N. Kawaguchi, T. Yanagida, Development of Tl-doped KI single crystal scintillators, Radiat. Phys. Chem. 207 (2023) 110820, https://doi.org/10.1016/j.radphyschem.2023.110820.

[5] Y. Syrotych, V. Gorbenko, J. Pejchal, R. Kucerkova, J.A. Mares, M. Nikl, et al., Two- and three-layered composite scintillators based on the Ce3+-doped GAGG and TbAG garnets for the simultaneous registration of various types of ionizing radiation, Cryst. Growth Des. 24 (2024) 6954–6964, https://doi.org/10.1021/acs.cgd.4c00252.

[6] C.J. Salas-Juárez, M.A. Ugalde-Valdés, J. Guzmán-Mendoza, D. Nolasco-Altamirano, M. Martínez-Gil, C.E. Gómez-Dominguez, et al., Persistent luminescence of commercial TLD-100 dosimeter: using shallow traps for radiation dosimetry, Radiat. Meas. 167 (2023) 106997, https://doi.org/10.1016/j.radmeas.2023.106997.

[7] Y. Li, S. Xu, F. Meng, H. Jiang, S. Yao, X. Zhang, et al., Insight into the structural, mechanical and optical properties of NaCl:Tb crystals for the WLED and TLD applications, Ceram. Int. 49 (2023) 28274–28282, https://doi.org/10.1016/j.ceramint.2023.06.082.

[8] E. Aboelezz, B.W. Pogue, Review of nanomaterial advances for ionizing radiation dosimetry, Appl. Phys. Rev. 10 (2023) 021312, https://doi.org/10.1063/5.0134982.

[9] E. Nichelatti, M. Piccinini, P. Nenzi, L. Picardi, C. Ronsivalle, R.M. Montereali, Proton-beam energy diagnostics by color-center photoluminescence imaging in LiF crystals: implementation of multiple Coulomb scattering into an analytical Bragg-curve model, Nucl. Instrum. Methods Phys. Res. Sect. B Beam Interact.

Mater. Atoms 547 (2024) 165207, https://doi.org/10.1016/j.nimb.2023.165207.

[10] M. Khoshakhlagh, J. Islamian, S. Abedi, B. Mahmoudian, Development of scintillators in nuclear medicine, World J. Nucl. Med. 14 (2022) 156—159.

[11] K. Watanabe, Y. Kawabata, A. Yamazaki, A. Uritani, T. Iguchi, K. Fukuda, et al., Development of an optical fiber type detector using a Eu:LiCaAlF6 scintillator for neutron monitoring in boron neutron capture therapy, Nucl. Instrum. Methods Phys. Res. Sect. Accel. Spectrometers Detect. Assoc. Equip. 802 (2015) 1—4, https://doi.org/10.1016/j.nima.2015.08.056.

[12] N. Salah, P.D. Sahare, A.A. Rupasov, Thermoluminescence of nanocrystalline LiF:Mg, Cu, P. J Lumin 124 (2007) 357—364, https://doi.org/10.1016/j.jlumin.2006.04.004.

[13] Y.S. Horowitz, Linearisation of the dose response of composite peak 5 in LiF:Mg,Ti by post-irradiation photon excitation, Phys. Med. Biol. 69 (2024), https://doi.org/10.1088/1361-6560/ad8298.

[14] S. Lee, J. Lee, G. Kim, S.J. Ye, Estimating 10B and 14N doses using a pair of LiF-based TLD-600 and TLD-700 as an alternative to gold activation method, Nucl. Instrum. Methods Phys. Res. Sect. Accel. Spectrometers Detect. Assoc. Equip. 1050 (2023), https://doi.org/10.1016/j.nima.2023.168141.

[15] Y.S. Horowitz, L. Oster, I. Eliyahu, The saga of the thermoluminescence (TL) mechanisms and dosimetric characteristics of LiF: Mg,Ti (TLD-100), J. Lumin. 214 (2019) 116527, https://doi.org/10.1016/j.jlumin.2019.116527.

[16] M. Behmadi, S. Mohammadi, M.E. Ravari, A. Mohammadi, M.E. Loushab, M.T. Bahreyni Toossi, M. Ghergherehchi, Neutron dosimetry with a pair of TLDs for the elekta precise medical linac and the evaluation of optimum moderator thickness for the conversion of fast to thermal neutrons, Nucl. Eng. Technol. 56 (2024) 753—761, https://doi.org/10.1016/j.net.2023.11.014.

[17] M.D. Baker, A.D. Baker, C.R.H. Hanusa, K. Paltoo, E. Danzig, J. Belanger, Bonding in sodium chloride nanotubes: a new analysis via madelung constants and cohesive energies, J. Phys. Chem. C 117 (2013) 25742—25747, https://doi.org/10.1021/jp405978d.

[18] F.A. Fernandez-Lima, A.V. Henkes, E.F. da Silveira, M.A.C. Nascimento, Alkali halide nanotubes: structure and stability, J. Phys. Chem. C Nanomater. Interfaces 116 (2012), https://doi.org/10.1021/jp208090j.

[19] F. Froborg, A. Duffy, Annual modulation in direct dark matter searches, J. Phys. G Nucl. Part. Phys. 47 (2020), https://doi.org/10.1088/1361-6471/ab8e93.

[20] C.J. Hailey, W.W. Craig, F.A. Harrison, J. Hong, K. Mori, J. Koglin, H. T. Yu, K.P. Ziock, Development of the gaseous antiparticle spectrometer for space-based antimatter detection, Nucl. Instrum. Methods Phys. Res. Sect. B Beam Interact. Mater. Atoms 214 (2004) 122—125, https://doi.org/10.1016/j.nimb.2003.08.004.

[21] K. Shunkeyev, A. Tilep, S. Sagimbayeva, Z. Ubaev, A. Lushchik, The effect of instability of KCl:Na single crystals, Crystals 13 (2023), https://doi.org/10.3390/cryst13020364.

[22] K. Shunkeyev, A. Tilep, Sh Sagimbayeva, A. Lushchik, Z. Ubaev, L. Myasnikova, N. Zhanturina, Zh Aimaganbetova, The enhancement of exciton-like luminescence in KCl single crystals under local and uniaxial elastic lattice deformation, Nucl. Instrum. Methods Phys. Res. Sect. B Beam Interact. Mater. Atoms 528 (2022) 20—26, https://doi.org/10.1016/j.nimb.2022.08.002.

[23] K. Shunkeyev, Z. Aimaganbetova, L. Myasnikova, A. Maratova, Zh Ubaev, Mechanisms of radiation defect formation in KCl crystals under the influence of local and plastic deformation, Nucl. Instrum. Methods Phys. Res. Sect. B Beam Interact. Mater. Atoms 509 (2021) 7—11, https://doi.org/10.1016/j.nimb.2021.10.010.

[24] K. Shunkeyev, A. Lushchik, L. Myasnikova, Sh Sagimbaeva, Zh Ubaev, Z. Aimaganbetova, Deformation-stimulated ex luminescence in a RbI single crystal, Low Temp. Phys. 45 (2019) 1127—1130, https://doi.org/10.1063/1.5125992.

[25] A. Elango, Sh Sagimbaeva, E. Sarmukhanov, T. Savikhina, K. Shunkeev, Effect of uniaxial stress on luminescence of X- and VUV-irradiated NaCl and NaBr crystals, Radiat. Meas. 33 (2001) 823—827, https://doi.org/10.1016/S1350-4487(01)00244-X.

[26] A. Bekeshev, K. Shunkeev, E. Vasil'chenko, A. Elango, Effect of uniaxial compression on the luminescence of self-trapped excitons in CsI at 80 K, Phys. Solid State 39 (1997) 75—76, https://doi.org/10.1134/1.1129835.

[27] A. Lushchik, Ch Lushchik, V. Nagirnyi, E. Shablonin, E. Vasil'chenko, Low-temperature creation of Frenkel defects via hot electron-hole recombination in highly pure NaCl single crystal, Low Temp. Phys. 42 (2016) 547—551, https://doi.org/10.1063/1.4959011.

[28] M. Grinberg, Excited states dynamics under high pressure in lanthanide-doped solids, J. Lumin. 131 (2011) 433—437, https://doi.org/10.1016/j.jlumin.2010.10.043.

[29] S. Mahlik, High-pressure study of phosphors emission, in: Phosphor Handbook: Experimental Methods for Phosphor Evaluation and Characterization, 2022, pp. 419—445.

[30] M. Ramirez, L. Bausa, S.W. Biernacki, A. Kaminska, A. Suchocki, M. Grinberg, Influence of hydrostatic pressure on radiative transition probability of the intrashell 4f transitions in Yb ions in lithium niobate crystals, Phys. Rev. B 72 (2005) 224104, https://doi.org/10.1103/PhysRevB.72.224104.

[31] D.G. Schoemaker, Hyperfine components of VK centers, Phys. Rev. B 7 (1973) 786—801, https://doi.org/10.1103/PhysRevB.7.786.

[32] T.G. Castner, W. Känzig, The electronic structure of V-centers, J. Phys. Chem. Solid. 3 (1957) 178—195, https://doi.org/10.1016/0022-3697(57)90023-9.

[33] C. Lushchik, A. Lushchik, Decay of Electronic Excitations with Defect Formation in Solids, Nauka, 1989. ISBN: 978-5-02-014026-4.

[34] K. Shunkeyev, A. Kenzhebayeva, A. Krasnikov, V. Nagirnyi, Sh Sagimbayeva, D. Sergeyev, A. Tilep, Zh Ubaev, A. Lushchik, Luminescence of bound excitons created near sodium impurity ions in KCl:Na single crystals, Opt. Mater. X 25 (2025) 100395, https://doi.org/10.1016/j.omx.2024.100395.

[35] D.E. Aboltin, V.J. Grabovskis, A.R. Kangro, Ch Lushchik, A.A. O'Konnel-Bronin, I.K. Vitol, V.E. Zirap, Thermally stimulated and tunneling luminescence and frenkel defect recombination in KCl and KBr at 4.2 to 77 K, Phys. Status Solidi A 47 (1978) 667—675, https://doi.org/10.1002/pssa.2210470239.

[36] A.A. Elango, T.N. Nurakhmetov, Structure and generation mechanism of Br centres in X-rayed KBr, Phys. Status Solidi B 78 (1976) 529—536, https://doi.org/10.1002/pssb.2220780211.

[37] J. Manam, V.V. Ratnam, Effect of post-irradiation deformation on the thermally stimulated luminescence spectra of KCl:Na crystals, Nucl. Tracks Radiat. Meas. 10 (1982) 97—100, https://doi.org/10.1016/0735-245X(85)90015-8.

[38] K. Shunkeyev, S. Sagimbayeva, L. Myasnikova, A. Istlyaup, A. Kenzhebayeva, High-temperature thermally stimulated luminescence of the NaCl and NaCl-Li crystals, Eurasian J. Phys. Funct. Mater. 8 (2024) 71—78, https://doi.org/10.69912/2616-8537.1188.

[39] M. Ikezawa, T. Kojima, Luminescence of alkali halide crystals induced by UV-light at low temperature, J. Phys. Soc. Jpn. 27 (1969) 1551—1563, https://doi.org/10.1143/JPSJ.27.1551.

[40] C. Lushchik, J. Kolk, A. Lushchik, N. Lushchik, M. Taiirov, E. Vasilchenko, Decay of excitons into long-lived F,H and α,I pairs in KCl, Phys. Status Solidi B 114 (1982) 103—111.

[41] A. Lushchik, C. Lushchik, N. Lushchik, A. Frorip, O. Nikiforova, Formation and decay of electronic excitations localized near divacancies in alkali halides, Phys. Status Solidi B 168 (1991) 413—423, https://doi.org/10.1002/pssb.2221680204.

[42] N. Itoh, Interstitial and trapped-hole centers in alkali halides, Cryst. Lattice Defects 3 (1972) 115—143.

[43] K. Shunkeyev, L. Myasnikova, A. Barmina, N. Zhanturina, S. Sagimbayeva, Z. Aimaganbetova, D. Sergeyev, The thermostimulated luminescence of radiation defects in KCl, KBr and KI crystals at elastic and plastic deformation, J. Phys. Conf. Ser. 830 (2017) 012138, https://doi.org/10.1088/1742-6596/830/1/012138.

[44] K. Shunkeyev, D. Sergeyev, W. Drozdowski, K. Brylev, L. Myasnikova, A. Barmina, N. Zhanturina, S. Sagimbayeva, Z. Aimaganbetova, The deformation stimulated luminescence in KCl,

KBr and KI crystals, J. Phys. Conf. Ser. 830 (2017) 012139, https://doi.org/10.1088/1742-6596/830/1/012139.

[45] C.G. Reddy, K.N. Reddy, Effect of plastic deformation on the thermally stimulated luminescence of NaCl:Y crystals, Mater. Chem. Phys. 27 (1991) 325—329, https://doi.org/10.1016/0254-0584(91)90129-I.

[46] ACh Lushchik, A.G. Frorip, Thermalized and hot interstitial halogen ions in alkali halides, Phys. Status Solidi B 161 (1990) 525—535, https://doi.org/10.1002/pssb.2221610208.

[47] J. Aluker, D. Lusis, S. Chernov, Jelektronnye Vozbujdenija I Radioluminescencija Shhelochno-Galoidnyh Kristallov, Zinatne, 1979 (In Russian).

[48] P. Varotsos, K. Alexopoulos, Calculation of the migration volume of vacancies in ionic solids from macroscopic parameters, Phys. Status Solidi A 47 (2) (1978) 797, https://doi.org/10.1515/9783112501108-059.

[49] M. Beniere, M. Chemla, F. Beniere, Vacancy pairs and correlation effects in KCl and NaCl single crystals, J. Phys. Chem. Solid. 37 (1976) 525—538, https://doi.org/10.1016/0022-3697(76)90080-9.

[50] P. Varotsos, K. Alexopoulos, On the question of the calculation of migration volumes in ionic crystals, Philos. Mag. A 42 (1980) 13—18, https://doi.org/10.1080/01418618008239352.